Multifunctional optical nanofiber polarization devices with 3D geometry

Jin-hui Chen, Ye Chen, Wei Luo, Jun-long Kou, Fei Xu,* and Yan-qing Lu

National Laboratory of Solid State Microstructures and College of Engineering and Applied Sciences, Nanjing University, Nanjing 210093, China

feixu@nju.edu.cn

Abstract: Here a reliable fabrication process enabling the integration of multiple functions in a single rod with one optical nano/microfiber (ONM) was proposed, which represents a further step in the "lab-on-a-rod" technology roadmap. With a unique 3D geometry, the all-fiber in-line devices based on lab-on-a-rod techniques have more freedom and potential for compactness and functionality than conventional fiber devices. With the hybrid polymer–metal–dielectric nanostructure, the coupling between the plasmonic and waveguide modes leads to hybridization of the fundamental mode and polarization-dependent loss. By functionalizing the rod surface with a nanoscale silver film and tuning the coil geometry, a broadband polarizer and single-polarization resonator, respectively, were demonstrated. The polarizer has an extinction ratio of more than 20 dB over a spectral range of 450 nm. The resonator has a Q factor of more than 78,000 with excellent suppression of polarization noise. This type of miniature single-polarization resonator is impossible to realize by conventional fabrication processes and has wide applications in fiber communication, lasing, and especially sensing.

©2014 Optical Society of America

OCIS codes: (060.2310) Fiber optics; (060.2340) Fiber optics components; (130.5440) Polarization-selective devices.

References and links

1. J. Simpson, R. Stolen, F. Sears, W. Pleibel, J. MacChesney, and R. Howard, "A single-polarization fiber," J. Lightwave Technol. **1**(2), 370–374 (1983).
2. D. A. Nolan, G. E. Berkey, M. J. Li, X. Chen, W. A. Wood, and L. A. Zenteno, "Single-polarization fiber with a high extinction ratio," Opt. Lett. **29**(16), 1855–1857 (2004).
3. R. B. Dyott, J. Bello, and V. A. Handerek, "Indium-coated D-shaped-fiber polarizer," Opt. Lett. **12**(4), 287–289 (1987).
4. K. Thyagarajan, S. Diggavi, A. K. Ghatak, W. Johnstone, G. Stewart, and B. Culshaw, "Thin-metal-clad waveguide polarizers: analysis and comparison with experiment," Opt. Lett. **15**(18), 1041–1043 (1990).
5. S. M. Tseng, S. P. Ma, K. F. Chen, and K. Y. Hsu, "Method for preparing fiber-optic polarizer," US Patent 5,781,675 (1998).
6. R. B. Dyott, R. Ulrich, and J. D. Meyer, "Optical fiber polarizer," US Patent 4,589,728, (1986).
7. Q. Bao, H. Zhang, B. Wang, Z. Ni, C. H. Y. X. Lim, Y. Wang, D. Y. Tang, and K. P. Loh, "Broadband graphene polarizer," Nat. Photon. **5**(7), 411–415 (2011).
8. Y. Chen, F. Xu, and Y. Q. Lu, "Teflon-coated microfiber resonator with weak temperature dependence," Opt. Express **19**(23), 22923–22928 (2011).
9. J. L. Kou, Y. Chen, F. Xu, and Y. Q. Lu, "Miniaturized broadband highly birefringent device with stereo rod-microfiber-air structure," Opt. Express **20**(27), 28431–28436 (2012).
10. M. Consales, A. Ricciardi, A. Crescitelli, E. Esposito, A. Cutolo, and A. Cusano, "Lab-on-fiber technology: toward multifunctional optical nanoprobes," ACS Nano **6**(4), 3163–3170 (2012).
11. P. B. Johnson and R.-W. Christy, "Optical constants of the noble metals," Phys. Rev. B **6**(12), 4370–4379 (1972).
12. R. F. Oulton, V. J. Sorger, D. Genov, D. Pile, and X. Zhang, "A hybrid plasmonic waveguide for subwavelength confinement and long-range propagation," Nat. Photon. **2**(8), 496–500 (2008).
13. R. Ismaeel, T. Lee, M. Ding, M. Belal, and G. Brambilla, "Optical microfiber passive components," Laser Photon. Rev. **7**(3), 350–384 (2013).
14. X. Guo, Y. Li, X. Jiang, and L. Tong, "Demonstration of critical coupling in microfiber loops wrapped around a copper rod," Appl. Phys. Lett. **91**, 073512 (2007).

#212818 - $15.00 USD Received 26 May 2014; revised 9 Jul 2014; accepted 10 Jul 2014; published 16 Jul 2014

15. F. Bonaccorso, Z. Sun, T. Hasan, and A. Ferrari, "Graphene photonics and optoelectronics," Nat. Photonics **4**(9), 611–622 (2010).

1. Introduction

Maintaining and manipulating the polarization state of light are of great importance in fiber systems including communication, sensor, and laser systems. Compared with bulk polarization-controlling devices, fiber-based polarization-controlling components (PCCs) have many advantages: easier alignment, smaller insertion loss, and compatibility with fiber systems. Numerous different types of fiber PCCs have been proposed and developed over the past decades. For example, the most important PCC, the in-line fiber polarizer, can be fabricated from specialized W-profile fibers [1] and hole-assisted fibers [2], or by coating a side-polished single-mode fiber (SMF) with a metallic thin film [3–5], birefringent polymers [6], or graphene [7]. These fabrication methods are either complicated or costly. Most of the fibers are too thick (diameter > 100 µm) to be bent into a small coil and have to be carefully kept as straight as possible to prevent additional birefringence. In real applications, different single-function PCCs have to be spliced or connected and carefully assembled as well as aligned to achieve optical performance. The system will inflate quickly and is sensitive to external perturbations such as changes in position and temperature, and bending or twisting of the fiber pigtails. Moreover, it is also very difficult to combine multiple functions in one component such as a miniature single-polarization resonator, which is important for rotation and current sensing.

On the other hand, 3D micro/nanodevices based on silica (optical nano/microfiber, ONM) have attracted increasing attention because of the recent rapid development of the so-called wrap-on-a-rod technology [8, 9]. Because they are fabricated from an SMF with low stiffness and micrometric bending radii, ONMs can be wrapped multiple times on a thin rod (hundreds of micrometers) and do not experience any input/output coupling problems. Unlike conventional one-dimension fiber devices, they have a unique 3D geometry that is more compact, flexible, and extensible. Recently, a variety of 3D ONM devices have been presented or demonstrated, including a resonator, a grating, and a Hi-Bi ONM. By tuning the pitch between turns and specializing the rod surface, multiple functions can be integrated on a single device, which is the concept of the future lab-on-a-rod, similar to lab-on-fiber [10]. Here we have to emphasize that only the rod surface needs to be functionalized with different materials and micro/nanostructures, and it is not necessary to treat the thin ONM, which is more challenging. In this context, we tried to integrate polarization-related functions on a rod by the wrap-on-a-rod technique. First, a thin polymer rod is functionalized with a nanoscale silver film, and an in-line broadband polarizer based on decoupled coiled ONMs on the rod can be obtained. A polarization extinction ratio of more than 20 dB can be evenly achieved in a wavelength range of ~450 nm. Then the coiled ONMs are adjusted for coupling, and the structure can yield a single-polarization resonator with a Q factor of greater than 78,000 and an average extinction ratio of greater than 10 dB around 1550 nm. The fabrication process is reliable and permits easy handling. The device is compact and stable. More complex functions such as lasing, filtering, and delaying can be integrated onto the rod by further design and processing of the coil geometry and the nanopattern on the rod surface.

2. Schematic of a polarization-related ONM Lab-on-a-rod device

Figure 1 illustrates the 3D structure of an ONM lab-on-a-rod device. A circular ONM is wrapped on a rod that is modified using different surface structures or materials. The rod serves only as a supporting element and can be made of any material as long as the surface is sufficiently smooth. We generally use a polymethyl methacrylate (PMMA) or silica rod. Multifunction integration can be realized by specializing the coil geometry and rod surface pattern. Here we functionalize a PMMA rod by coating it with a low-index polymer, Teflon (Teflon® AF 601S1-100-6, a production of DuPont) and a metal, silver. Teflon is first coated on the rod's surface to smooth it and avoid loss from the surface roughness and high refractive index of the PMMA rod. The nanoscale silver film serves as a polarization-

#212818 - $15.00 USD Received 26 May 2014; revised 9 Jul 2014; accepted 10 Jul 2014; published 16 Jul 2014
(C) 2014 OSA

dependent absorber. The pitches between adjacent turns can be tuned for different functions. When two coils are decoupled and far from each other, no energy is exchanged between the light propagating in the coils. A broadband in-line polarizer can be realized because of the difference in propagation loss for the transverse electric (TE) and transverse magnetic (TM) modes. In contrast, when two coils are sufficiently close, a strong coupling effect leads to light traveling from one to the other, and a single-polarization ONM resonator can be formed. Here we investigate both of these two extreme cases.

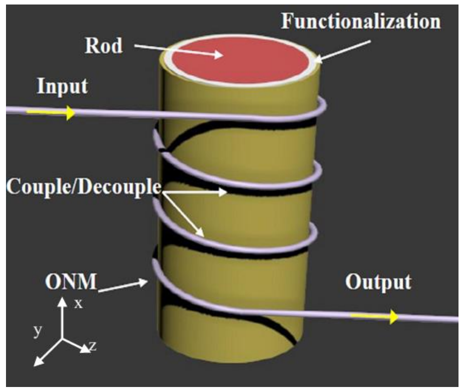

Fig. 1. Schematic of ONM lab-on-a-rod device. The rod surface is functionalized using nanostructure. The pitches between adjacent turns can be tuned for coupling or decoupling. Multifunction integration can be realized by modifying the rod surface and turn pitches. In our experiment, the PMMA (red) rod is coated with Teflon (white) and silver (yellow) films.

We employed the finite element method (FEM) to numerically investigate the polarization-related loss mechanism. Because the diameter of the ONM is far smaller than the diameter of the rod, we can ignore the bending effect, and the structure can be simplified [9], as illustrated in Fig. 2. The optical constants of silver were obtained from [11], and in all our calculation we considered the permittivity dispersion of silver and the fiber. In one type of hybrid plasmonic waveguide consisting of a dielectric nanowire touching a metal surface, coupling between the plasmonic and waveguide modes leads to hybridization of the fundamental mode and strong polarization-dependent characteristics. When light is input to the waveguide structure, two orthogonal TE and TM modes are excited, as shown in Fig. 2. For the TM mode, it can be coupled with the surface plasmon polaritons (SPPs) supported by the silver film and forms a hybrid mode [12], whereas the TE mode will be well confined in the core of the ONM, as shown in the inset of Fig. 2. As a result, the TM mode suffers a larger propagation loss than the TE mode, which makes our structure a TE mode pass polarizer. Because the diameter of the ONM is very large, the hybrid waveguide for the TM mode supports a low-loss cylinder mode compared to the loss of SPPs [12]. Figure 3(a) shows the theoretical calculation of the dependence of the propagation loss on the ONM radius and metal thickness. The loss increases monotonically with decreasing ONM radius r and metal thickness d, and the relevant slope increases quickly with the metal thickness. This is because the evanescent field of the ONM increases with the decrease in the ONM radius. Further, the coupling between the ONM core mode and SPPs supported by the silver film also increases with decreasing metal film thickness. The wavelength dependence of the propagation loss is shown in Fig. 3(b) for different ONMs at a metal thickness d = 100 nm. The curves are much flattened for both the TE and TM modes in the spectral range from 1200 to 1650 nm.

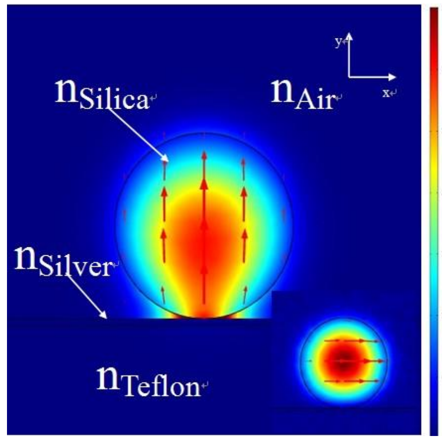

Fig. 2. Cross section and electric field distribution of hybrid plasmonic waveguide structure. Refractive indices of different materials are labeled in the figure. Red arrow indicates a thickness of 100 nm. The field is calculated at a wavelength of 1550 nm with the following parameters: $r_{ONM} = 1.5$ µm, $n_{air} = 1$, $n_{teflon} = 1.31$, $n_{silica} = 1.4443$, $\varepsilon_{silver} = -126 + 3.2i$ [11]. Inset: electric field distribution of the *x* polarization mode (TE mode).

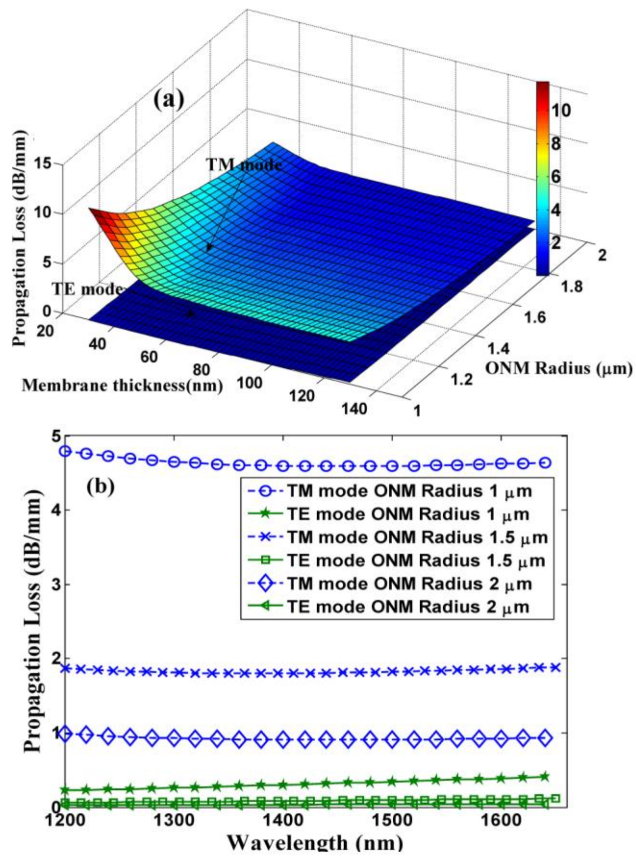

Fig. 3. Theoretical propagation loss for TE and TM modes versus metal thickness, ONM radius, and light wavelength. (a) Theoretical loss for TE and TM modes versus metal thickness and ONM radius at fixed light wavelength, $\lambda = 1550$ nm. (b) Theoretical propagation loss for TE and TM modes versus wavelength with varying radius, $r = 1$ µm, 1.5 µm, and 2 µm. Silver membrane thickness fixed at $d = 100$ nm.

#212818 - $15.00 USD Received 26 May 2014; revised 9 Jul 2014; accepted 10 Jul 2014; published 16 Jul 2014
(C) 2014 OSA

3. Functionalizing of rod surface and realization of polarization functions

In our experiment, the PMMA rod (2 mm in diameter) is dipped coated with Teflon tens of micrometers in thickness. Then a thin silver film with a thickness of approximately 100 nm is deposited on the rod by physical vapor deposition. The thickness of silver film is controlled by the deposition rate and time. We use a flame-brushing technique to draw an ONM from a conventional SMF. The radius of the average ONM is around 1~2 µm. Then the ONM is wrapped (two turns) around the silver-coated rod with the aid of a microscope and a rotational stage. The pitches between adjacent turns can be controlled for coupling or decoupling.

The polarization-related spectra in the near-infrared (1200–1650 nm) are measured by a wavelength scanning technique. Light from a broadband super-continuum source (NKT K91-120-02) is linearly polarized by a polarizer, and then a half-wave ($\lambda/2$) plate is used to continuously adjust the polarization axis of the incident beam. The transmission spectra of various samples are recorded by an optical spectrum analyzer (OSA, Yokogawa, AQ6370C). In the first polarizer experiment, different coils of the ONM are kept away from each other to prevent mutual field coupling. The inset in Fig. 4(a) shows an optical image of the two-turn ONM on the rod. The distance between the coils is ~100 µm. The two-turn structure indicates that the length of the ONM on the rod is 12.5 mm. The polarization-dependent spectra are shown in Fig. 4(a). As can be seen, a large extinction ratio (>20 dB) covering a 450 nm bandwidth is obtained, which indicates excellent maintenance of single polarization. However, the noise in the spectrum increases when the wavelength is below ~1300 nm, which is attributed to the fact that at these wavelengths, the fiber pigtail becomes multi-mode. The insertion loss of our device is approximately 6 dB, which can be attributed to the eigenmode loss and surface scattering loss. We notice that for the TM mode, the output spectra showed an interference pattern with a free spectral range (FSR) amounting to 140 nm. This is because of the high birefringence of the system and the imperfect alignment between the input polarization light and the TM mode [9]. We also conduct a control experiment in which the ONM is wrapped around a Teflon-coated PMMA rod, which shows no polarizing effect, as shown in Fig. 4(a). Figure 4(b) presents a polar image measured at 1400 nm with an extinction ratio of 23 dB, which agrees well with the data in Fig. 4(a).

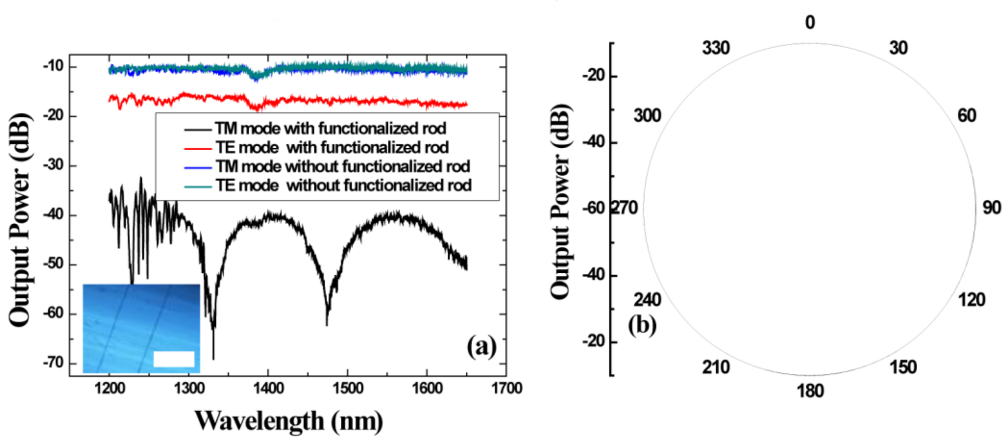

Fig. 4. Broadband polarizing. (a) Polarization measurements conducted at wavelengths of 1200–1650 nm (L_{ONM} = 12.5 mm). The output maximum (red area) and minimum (black area) were recorded at polarization angles θ = 90° (TE mode) and θ = 0° (TM mode). Blue and cyan lines indicate ONMs wrapped on Teflon-coated rod, which show no polarizing effect. Inset: Optical microscopic picture of the sample and the scale bar is 100µm. (b) Polar image measured at 1400 nm.

Without loss of generality, we select numerical results at a wavelength of 1400 nm to compare with the experimental results. From Fig. 3(b), the calculated extinction ratio is 1.72 dB/mm (@1400 nm), so the total extinction ratio amounts to 21.5 dB (L_{ONM} = 12.5 mm), which shows good agreement with the experimental result (23 dB). Moreover, the extinction ratio will be increased much further as the number of turns of the ONM coil increases, and the insertion loss of the device will be inevitably increased. To some degrees, increasing the diameter of the rod is equivalent to increasing the number of ONM coils. However, if the diameter of the rod is too small and reach the critical bending radius of ONM, the bending loss of will be greatly multiplied, and a rod with smaller radius of curvature will also increase the difficulties of depositing uniform silver film.

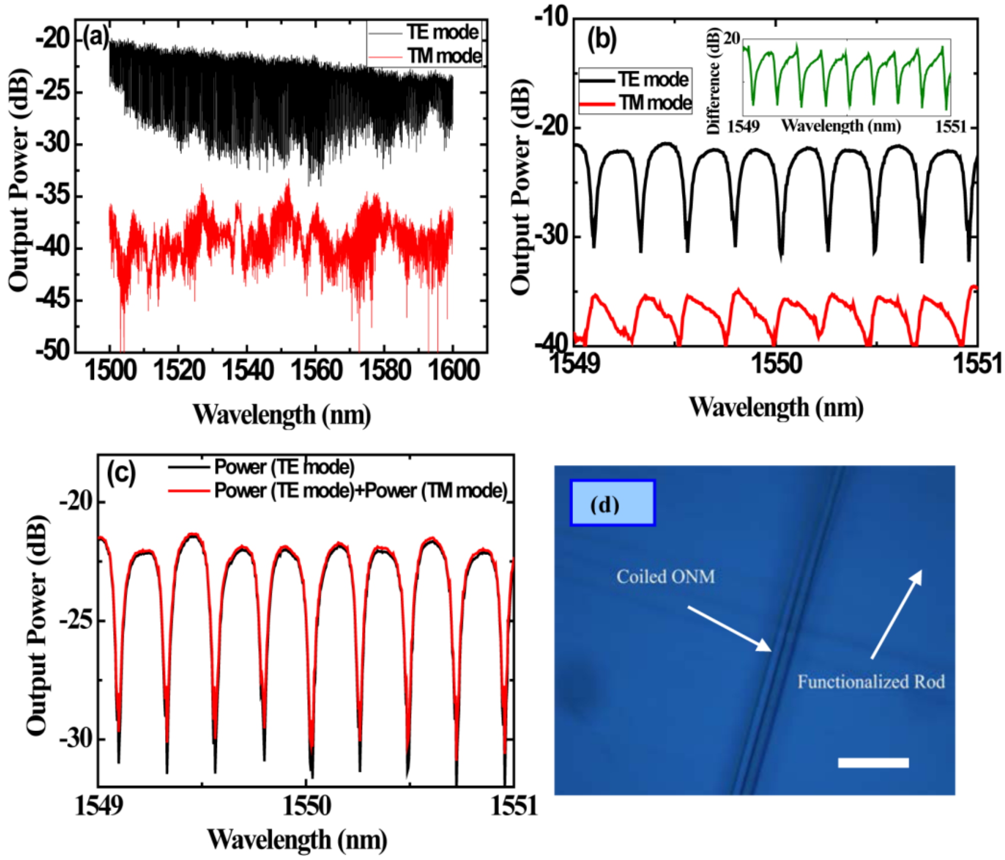

Fig. 5. Single-polarization single-mode resonator. (a) Transmission spectrum of a coil resonator as recorded from an optical spectrum analyzer. (b) Transmission spectrum around 1550 nm. Inset: The difference between TE mode and TM modes. (c) The output spectrum of TE mode and TE + TM mode, which is obtained from (b). (d) Optical image of sample, the scale bar is 20μm. The two turns of the MF were almost touching each other and formed a resonator.

When the adjacent coils of the ONM are sufficiently close, it forms a single-polarization single-mode resonator [13, 14]. We carefully wrap two turns of an ONM around the silver-coated rod with the help of microscope to make sure that the coils of the ONM are close to each other for coupling, as illustrated in Fig. 5(d). In Fig. 5(a), we showed the transmission spectra of the coil resonator for two orthogonal modes (TE and TM) as recorded from an optical spectrum analyzer. It is natural that the spectra of the two modes are separated because they suffer different propagation losses. From Fig. 5(b), we can find that around 1550 nm, the FSR is 0.24 nm, which agrees well with our theoretical calculation, and its full width at half-maximum is <0.02 nm, which is limited by the OSA resolution. Thus, the Q factor and finesse of our device are greater than 78,000 and 12, respectively. The inset of Fig. 5(b) shows the extinction ratio difference between TE and TM modes, the average value is about 10 dB. To illustrate the excellence of suppression of polarization noise of the device, we compared the output power of TE mode and TE + TM mode, as shown in Fig. 5(c). It is clearly demonstrated that the output TM mode power has little influence on TE mode even the input power for TE and TM modes are the same.

In most applications, the input linearly polarized light can be set to excite the TE mode. The polarization related coupling and instability, which are mainly from the fluctuation of fiber geometry and environment, can be suppressed well in the resonator, which is especially attractive for certain specialized applications such as gyros and current sensors. These functions cannot be realized in a one-dimensional fiber system. The Q factor can be increased by optimizing these parameters to tune the coupling coefficient and decrease the loss of the TE mode. Obviously, more polarization-related functions can be integrated with a compact size for future lab-on-a-rod devices.

4. Conclusion

We propose a new approach, the lab-on-a-rod, for polarization-related multifunction integration on a single rod by one ONM. The device has a unique 3D geometry obtained by wrapping the ONM around the nanostructured rod. The nanostructuring procedure is performed only on the thick rod, rather than on the thin fiber [10], which simplifies fabrication.

Compared with conventional fiber polarization devices, this device offers more freedom and greater potential for compactness and functionality. Moreover, we present numerical simulations that investigate the polarization loss mechanism. By functionalizing the rod surface with a nanoscale silver film and tuning the pitches of the coils, a broadband polarizer and single-polarization resonator, respectively, are demonstrated. The polarizer has an extinction ratio of more than 20 dB over a wavelength range of 450 nm. A higher extinction ratio can be easily obtained by adding more turns. The resonator has a Q factor of >78,000 with excellent suppression of the polarization noise. A higher Q factor can be achieved by optimizing those parameters. This type of compact single-polarization resonator is impossible to realize with previously reported methods and has a number of applications in communications, nonlinear optics, and sensing. More polarization-related functions can be integrated with an ultracompact size for future lab-on-a-rod devices. The platform is also quite compatible with the emerging 2-D materials, such as graphene and MoS_2. These new material can introduce more functionalities to the fiber system, such as the nonlinear effect, mode locking, light-wave modulating etc. For instance, if we use graphene to modify the rod, the device may work over a larger bandwidth since the linear dispersion of the Dirac fermions enables graphene broad band applications [15]. Overall, our results demonstrate how the definition of viable lab-on-a-rod technologies would enable the realization of technological platforms completely integrated on a single rod with one ONM, for exploitation in many application fields.

Acknowledgments

This work is supported by National 973 program under contract No. 2012CB921803 and 2011CBA00205, National Science Fund for Excellent Young Scientists Fund (61322503) and National Science Fund for Distinguished Young Scholars (61225026).The authors also acknowledge the support from PAPD and the Fundamental Research Funds for the Central Universities, and the help on FEM simulation by Prof. Xiaoshun Jiang and Xuejing Zhang.